Intra-arterial high signals on arterial spin labeling perfusion images predict the occluded internal carotid artery segment

Shu Sogabe[1], Junichiro Satomi[1], Yoshiteru Tada[1], Yasuhisa Kanematsu[1], Kazuyuki Kuwayama[1], Kenji Yagi[1], Shotaro Yoshioka[1], Yoshifumi Mizobuchi[1], Hideo Mure[1], Izumi Yamaguchi[1], Takashi Abe[2], Nobuaki Yamamoto[3], Keiko T. Kitazato[1], Ryuji Kaji[3], Masafumi Harada[2], Shinji Nagahiro[1]

[1]Department of Neurosurgery, [2]Department of Radiology, [3]Department of Clinical Neurosciences, Institute of Biomedical Biosciences, Tokushima University Graduate School, Tokushima, Japan

Address for correspondence:

Junichiro Satomi, MD, PhD

Department of Neurosurgery

Institute of Biomedical Biosciences

Tokushima University Graduate School

3-18-15, Kuramoto-cho, Tokushima 770-8503, Japan

Tel: +81-88-633-7149; Fax: +81-88-632-9464

E-mail: junichirosatomi@gmail.com

Word count: 5428 words

Number of Figures: 4

Number of Tables: 2

The authors' contribution to the manuscript

Shu Sogabe, Junichiro Satomi, Yoshiteru Tada, Keiko T. Kitazato: Manuscript writing

Yasuhisa Kanematsu, Kazuyuki Kuwayama, Kenji Yagi, Shotaro Yoshioka, Izumi Yamaguchi, Nobuaki Yamamoto: Data collection

Takashi Abe, Masafumi Harada, Yoshifumi Mizobuchi, Hideo Mure: Image analysis

Shinji Nagahiro, Ryuji Kaji: Project development

Ethical approval

All procedures performed in studies involving human participants were in accordance with the ethical standards of the institutional and/or national research committee and with the 1964 Helsinki declaration and its later amendments or comparable ethical standards. For this type of study formal consent is not required. This article does not contain any studies with animals performed by any of the authors.

Informed consent

Additional informed consent was obtained from all individual participants for whom identifying information is included in this article.

Conflict of interest statement

We declare that we have no conflict of interest.

Acknowledgement

We thank the members of the Stroke Care Unit of Tokushima University Hospital for their contributions to this work.

Abstract

Introduction

Arterial spin labeling (ASL) involves perfusion imaging using the inverted magnetization of arterial water. If the arterial arrival times are longer than the post-labeling delay, labeled spins are visible on ASL images as bright intra-arterial high signals (IASs); such signals were found within occluded vessels of patients with acute ischemic stroke. The identification of the occluded segment in the internal carotid artery (ICA) is crucial for endovascular treatment. We tested our hypothesis that IASs on ASL images can predict the occluded segment.

Methods

Our study included 13 patients with acute ICA occlusion who had undergone angiographic and ASL studies within 48 hr of onset. We retrospectively identified the IAS on ASL images and angiograms and recorded the occluded segment and the number of IAS-positive slices on ASL images. The ICA segments were classified as cervical (C1), petrous (C2), cavernous (C3), and supraclinoid (C4).

Results

Of 7 patients with intracranial ICA occlusion, 5 demonstrated IASs at C1-C2, suggesting that IASs could identify stagnant flow proximal to the occluded segment. Among 6

patients with extracranial ICA occlusion, 5 presented with IASs at C3-C4, suggesting that signals could identify the collateral flow via the ophthalmic artery. None had IASs at C1-2. The mean number of IAS-positive slices was significantly higher in patients with intra- than extracranial ICA occlusion.

Conclusion

IASs on ASL images can identify slow stagnant- and collateral flow through the ophthalmic artery in patients with acute ICA occlusion and help to predict the occlusion site.

Key words: magnetic resonance imaging, arterial spin labeling, internal carotid artery occlusion, occluded segment

Introduction

Acute ischemic stroke due to acute internal carotid artery (ICA) occlusion is often associated with severe and persistent neurological deficits and a high mortality rate. Among stroke patients who received tissue plasminogen activator (tPA) therapy 71.3% had unfavorable outcomes, as did 79.4% who did not undergo thrombolysis (modified Rankin scale, mRS: 3-6) [1]. Four randomized controlled trials [2-5] showed that endovascular treatment was superior to intravenous recombinant tPA (iv-rtPA) therapy alone and to standard care.

The outcome was worse in patients with acute intra- than extracranial ICA occlusion [6]. This may reflect a difference in the amount of collateral circulation. Intracranial ICA occlusion tends to be treated endovascularly with Merci thrombectomy (Stryker), a penumbra system (Penumbra, Inc.) or a stent retriever [Solitaire (Covidien), Trevo (Stryker)]. As the endovascular treatment of extracranial ICA occlusion first requires angioplasty by balloon or stent, the occluded segment must be known before such therapy. However, magnetic resonance angiography (MRA) cannot be used to diagnose the occluded ICA segment because all signals disappear.

With arterial spin labeling (ASL), perfusion can be visualized and the cerebral blood flow (CBF) can be quantified. ASL uses magnetically labeled arterial blood water protons as endogenous tracer particles [7, 8]. If the arterial arrival time exceeds the post-labeling delay, labeled spins are visible as bright intra-arterial high signals (IASs) known as the arterial transit artifact [9]. The post-labeling delay time defines the time required for spins to travel from the labeling plane or volume to the imaged slice; typically it is between 1,500 and 2,000 ms. Bright intravascular signals, attributable to slow-flowing blood on ASL images, have been observed upstream of major vessel occlusion sites [10, 11].

Based on these findings, we hypothesized that the detection of stagnant flow using a sequence other than MRA would be useful to identify the occluded ICA segment. We investigated whether IASs on ASL images help to distinguish between acute intracranial- and extracranial ICA occlusion and compared differences in the flow pattern, the location of IASs, and the length of IASs-positive sites in patients with acute ICA occlusion. Here we show that IASs are useful for identifying the occlusion site.

Methods

Subjects

Our institutional review board approved this retrospective study. Written informed consent was obtained from all patients or their relatives. Unless contraindicated, assessment with 3T magnetic resonance imaging (MRI) is the first-line diagnostic tool for stroke patients in our center. On March 1, 2012 we added ASL to the MRI protocol. From March 1, 2012 to July 31, 2015, 572 consecutive patients with acute ischemic stroke or transient ischemic attacks were admitted to our stroke care unit. Of these, 55 with acute ICA occlusion were seen within 48 hr after stroke onset; 37 patients underwent MRI and a good ASL image was acquired. In 13 patients we were able to diagnose the ICA occlusion segment on post-ASL angiographs; these patients are the study subjects in our retrospective study.

Clinical backgrounds and characteristics

The patients' age, sex, National Institutes of Health Stroke Scale (NIHSS) score at admission, the score based on diffusion weighted imaging - the Alberta Stroke Program Early Computed Tomography Score (DWI-ASPECTS [12]), their vascular risk factors including atrial fibrillation, hypertension, diabetes mellitus, and dyslipidemia, the time from onset to MRI, and the time from MRI to angiography were recorded. The stroke etiology was assessed based on the classification of Adams et al. [13].

MRI examination

MRI studies were acquired on a 3T MRI scanner (Discovery MR 750; GE Healthcare, Milwaukee, WI) equipped with an 8-channel phased-array head coil. For ASL we followed the method of Dai et al. [14].

ASL perfusion imaging was performed with pseudo-continuous labeling, background suppression, and a stack-of-spirals 3D fast spin echo imaging sequence. The parameters for ASL imaging were 512 sampling points on 8 spirals, field of view (FOV) 24 cm, reconstructed matrix 64 x 64, TR 4632 ms, TE 10.5 ms, NEX 2, labeling duration 1500 ms, post-labeling delay 1525 ms, slice thickness 4 mm, number of slices 36, total acquisition time 3 min 30 sec. For MRA they were FOV 22 cm, matrix 512 x 224, TR 30 ms, TE 2.8 ms, flip angle 17°, slice thickness 1.2 mm, number of slices 66.

Image analysis

IASs were defined as spot-like or vessel-like bright hyperintensity areas within an artery on ASL images (Figs. 1Ba-d). The ICA segments were classified as C1: cervical-, C2: petrous-, C3: cavernous-, C4: supraclinoid (Gibo et al. [15]). To determine the ICA segment harboring the slice visualized on ASL images we referred to the contralateral normal ICA on MRA images.

Two neuroradiologists who were not involved in the care of the patients independently reviewed all ASL data for the presence or absence of IASs and the involved ICA segment. They were blinded to clinical information and angiographic data. Their judgments were used to calculate inter-rater agreement. The recorded consensus judgments reflected the unanimous decision of the 2 neuroradiologists plus 2 other readers. IASs were recorded as present only by unanimous decision. If there was disagreement, IASs were judged as absent. The involved ICA segment was also identified only on the basis of a unanimous decision by the 4 readers. The consensus judgments returned for ASL findings were used for further analysis. IASs were assessed based on ASL studies performed at the time of admission. Acute ICA occlusion was diagnosed when the artery was invisible on MRA images and when there were symptoms compatible with the non-visualized artery.

Statistical analysis

Statistical analysis was performed using SPSS (IBM Statistics 22) with standard statistics. Inter-rater agreement for identifying IASs and the ICA segment was assessed using kappa (κ) statistics. Chi-square analysis or Fisher's exact test was used to compare binary variables. The Mann-Whitney *U* test was used to compare differences in the mean number of IASs. Values are expressed as the median (first to third interquartile). Statistical differences were considered significant at $p < 0.05$.

Results

Patient characteristics, site of ICA occlusion, and treatment

The median age of our 13 study subjects was 76 years (interquartile range 70-84 years), 3 were female, the median NIHSS score at presentation was 15 (12-18), and the median interval from onset to MRI was 406 min (269-645) (Table 1). ASL images of all 13 patients showed hypoperfusion in the MCA territory and the median DWI-ASPECTS was 9 (8-11), indicating a large ischemic penumbra in all patients. The occluded segment was intracranial in 7 patients (C2-, C3-, C4 segment of the ICA); 6 underwent embolectomy. Of the 6 patients with extracranial (C1) occlusion, 2 received iv-rtPA treatment and in 5 a carotid artery stent was placed before other procedures. Hypertension was diagnosed in 9 patients (intracranial ICA occlusion: n = 6, extracranial ICA occlusion: n = 3), atrial fibrillation in 4 (intracranial ICA occlusion: n = 3, extracranial ICA occlusion: n = 1), diabetes mellitus in 3 (intracranial ICA occlusion: n = 2, extracranial ICA occlusion: n = 1), and dyslipidemia in 2 (intracranial ICA occlusion: n = 1, extracranial ICA occlusion: n = 1). Patients with intracranial ICA occlusion tended to have a higher incidence of risk factors.

Inter-observer agreement for IAS detection

Two neuroradiologists, not involved in the care of patients, independently reviewed all ASL data for the presence or absence of IASs. Inter-observer agreement for the evaluation of IASs was excellent ($\kappa = 0.97$).

Angiographic and ASL findings in patients with intracranial ICA occlusion

MRA images of the 7 patients with intracranial ICA occlusion were inspected for the presence of ICA signals. All affected ICA signal in 6/7 cases were not identified except only a single patient who presented with occlusion in the C4 segment. Thus, MRA alone was inadequate for the prediction of the occluded ICA segment. The angiographic pattern on digital subtraction angiography (DSA) images was different among our 7 patients with intracranial ICA occlusion; 5 presented with C4 occlusion (cases 1-5) and 2 with occlusion below C3 (cases 6 and 7).

C4 segmental occlusion: The occlusion site in 5 of 7 patients (71%) with intracranial ICA occlusion was at the C4 segment. Figure 1 shows representative MRI and DSA findings in patients with C4 segmental occlusion. The DWI-ASPECTS was 8 (Fig. 1Aa) and ASL revealed reduced perfusion in all of the MCA territory (Fig. 1Ab). Figure 1B shows DSA images obtained in the early and late phases. On angiographs, the left intracranial ICA (C4) was occluded from just above the origin of the posterior communicating artery (PcomA) (Figs. 1Ba and 1Bb). We observed patency at the origin of the ICA and slow stagnant flow along the ICA extra- to intracranially into the ophthalmic artery and the PcomA. All 5 patients with C4 occlusion manifested slow flow along the ICA from the extra- to the intracranial ICA on DSA images. Figure 1Bc presents schemas of the occlusion site and the blood flow on angiographs; in Figure 1C, we present ASL images showing IASs within the C1-C4 segments of the left ICA, reflecting slow stagnant flow within the ICA. Figure 1D shows schemas of the occlusion site on angiographs and the area positive for IASs on ASL images.

Occlusion at sites lower than C3: The occlusion site in 2 of 7 (29%) patients with intracranial ICA occlusion was in a segment lower than C3. Figure 2 presents examples of MRI and DSA findings. The DWI-ASPECTS was 10 (Fig. 2Aa) and ASL showed reduced perfusion in all of the MCA territory (Fig. 2Ab). DSA images obtained in the early and late phases are shown in Figure 2B. Angiography revealed occlusion of the left ICA (C3) and collateral flow through the ophthalmic artery in the late phase (Figs. 2Ba and 2Bb). Although the origin of the ICA was patent, we observed ICA flow arrest because there was no outflow. Anterograde flow in the ICA through the ophthalmic artery was slow. The schemas in Figure 2Bc show the occlusion site and the blood flow on angiographs. On ASL images there were IASs within the C4 segment of the left ICA, reflecting anterograde flow in the ICA through the ophthalmic artery (Fig. 2C). Schemas of the occlusion site and the area positive for IASs on ASL images are presented in Figure 2D. In another patient with occlusion lower than the C3 segment we obtained the same DSA findings.

Angiographic and ASL findings in patients with extracranial ICA occlusion

There were 6 patients with extracranial ICA occlusion. On MRA images all ICA signals were not identified in all cases. Figure 3 shows representative MRI and DSA findings in patients with extracranial ICA occlusion. DWI and ASL scans revealed a large ischemic penumbra in the MCA territory (Figs. 3Aa and 3Ab). On angiographs we observed occlusion at the left ICA origin (C1) (Fig. 3Ba). Before balloon-angioplasty at the origin of the ICA we noted slow ante- and retrograde flow in the ICA through the ophthalmic artery (Fig. 3Ba); after balloon-angioplasty there was recanalization above the ICA origin (Fig. 3Bb). Schemas showing the occlusion site and the blood flow pattern on angiographs are presented in Figure 3Bc. ASL obtained before balloon-angioplasty detected IASs in the C3-C4 segments of the left ICA, reflecting slow ante- and retrograde flow through the ophthalmic artery (Fig. 3C). Schemas of the occlusion site and the area positive for IASs on ASL images are presented in Figure 3D. Among 6 patients with extracranial ICA occlusion, 5 manifested collateral flow in a short length of the ICA from C3 to C4 through the ophthalmic artery. No patients with extracranial ICA occlusion demonstrated stagnant flow in the C1-C2 segments of the ICA.

IAS-positive slices on ASL images at each occluded segment

Our angiographic findings indicate that the range and site of stagnant and slow flow within the ICA differed in patients with intracranial- and extracranial ICA occlusion. Therefore, we examined the relationship between the number and location of IAS-positive slices and the occluded ICA segment to determine whether IASs on ASL images differentiated between intra- and extracranial ICA occlusion.

Figure 4 shows the number of slices and the IAS-positive segment in patients with intra- and extracranial ICA occlusion. The number of IAS-positive slices was significantly higher in the former (average 8.3 vs. 2.0 slices: $p < 0.05$). This observation is consistent with angiographic findings that patients with intracranial ICA occlusion manifested a wide range of stagnant- and slow flow in the ICA. No IASs were observed at C1 and C2 in patients with extracranial ICA occlusion.

Accuracy and value of IASs at C1-C2 on ASL images for diagnosing intracranial ICA occlusion

Based on angiographic evidence for stagnant flow in the C1-C2 segments of the ICA, we hypothesized that IASs in these segments were predictive of intracranial ICA occlusion. Table 2 shows the value of IASs at the C1-C2 segments on ASL images for a diagnosis of intracranial ICA occlusion. The IAS-positive ratio in C1-C2 segments was significantly higher in patients with intra- than extracranial ICA occlusion (5/7 vs. 0/6). The sensitivity, specificity, positive- and negative predictive value, and the accuracy of these IASs was 71%, 100%, 100%, 75%, and 85%, respectively, indicating that IASs at the C1-C2 segments of the ICA are predictors of intracranial ICA occlusion.

Discussion

We found that almost all patients with intracranial ICA occlusion manifested slow stagnant flow in the C1-C4 segments of the ICA on DSA images; patients whose ICA occlusion was extracranial showed collateral flow in a narrow range (C3-C4) through the ophthalmic artery but no stagnant flow in the C1-C2 segments of the ICA. As on angiograms, we detected IASs in the C1-C4 segments on ASL images of patients with intracranial ICA occlusion. Notably, most of these patients manifested IASs not only in the C3-4- but also in the C1-C2 segments of the ICA. In contrast, in patients with extracranial ICA occlusion, we detected IASs in the C3-C4 segments. These observations indicate that IASs on ASL studies reveal slow stagnant- or collateral flow in patients with acute ICA occlusion and help to identify the occlusion site.

The endovascular treatment of patients with acute ICA occlusion has been successful. Saver et al. [5] reported that 47% of patients treated endovascularly had a favorable outcome (mRS 0-2). However, the therapeutic strategy to address intra- and extracranial ICA occlusion is different. In most patients with extracranial ICA occlusion, the occluded site was at the ICA origin and 83% of their patients required angioplasty; none with intracranial ICA occlusion did. Consequently, the preoperative prediction of the occlusion site is crucial to determine whether angioplasty at the origin of the ICA is required.

Elsewhere our group documented that in the presence of acute middle cerebral artery occlusion, the sensitivity of IASs is higher than the susceptibility vessel sign on T2*-gradient echo images [16]. However, no MRI findings demonstrating the occluded ICA segment have been reported. While the susceptibility vessel sign on T2*-gradient echo images can reveal acute endovascular clots in other vessels [17], susceptibility artifacts at the skull base or clots outside the scan range on such images make it difficult to detect this sign in patients with acute ICA occlusion. Due to the lack of ICA signals, MRA was not able to depict the occlusion site in the current study. While carotid ultrasound can distinguish between vessel occlusion and patency at the origin of the ICA, it requires special techniques and too much time in emergency situations. MRI, on the other hand, is useful for predicting the occluded site and in addition, it yields information such as the infarct volume and CBF.

We tested our hypothesis that IASs on ASL images are useful for detecting the occluded ICA segment. We now demonstrate that the sensitivity, specificity, and accuracy of IAS detection in the C1-C2 segments for a diagnosis of intracranial ICA occlusion were high (71%, 100%, and 85%, respectively). However, in 2 patients with intracranial ICA occlusion there were no IASs at C1-C2; the occluded- was lower than the C3 segment and angiographs showed flow arrest at C1-C2 and collateral flow through the ophthalmic artery. Anatomical features may explain this observation; under normal conditions, no vessels branch from the cervical (C1) segment of the ICA. The caroticotympanic and the vidian artery branch from the petrous (C2)- and the meningohypophyseal trunk and the inferolateral trunk branch off the cavernous (C3) segment of the ICA. The ophthalmic- and anterior choroidal artery, and the PcomA branch from the supraclinoid (C4) segment. As vessels branching from the C2-C3 segments are very small, they tend not to be visualized on angiographs. If the C2-C3 segment is occluded, vessels cannot provide collateral flow to the brain. This elicits flow arrest in the C1-C2 segments. We demonstrate that the presence of IASs in the C1-C2 segments is highly specific and useful for diagnosing intracranial ICA occlusion.

IASs and arterial transit artifacts are influenced by the post-labeling delay time [18]. Alsop et al. [19] recommended a post-labeling delay of 2000 ms for the accurate assessment of the CBF because a wide range of pathologies may not have been identified before imaging. A post-labeling delay of approximately 1500 ms has been applied in studies to investigate the presence and importance of intravascular high signals [11, 16]. As a longer post-labeling delay time on ASL studies detects slower flow [20], it may increase the sensitivity for IASs. Other imaging parameters such as the labeling approach, background suppression, and crusher gradients may affect the appearance of IASs on ASL studies. In our and earlier investigations, pseudo-continuous ASL (PCASL) was the labeling approach. The application of consecutive radiofrequency pulses on PCASL studies instead of a single short pulse or a limited number of pulses in pulsed ASL (PASL) and background suppression may show IASs more clearly. Crusher gradients are used for quantification by suppressing the intravascular signal. However, as they may remove important clinical information such as the presence of delayed flow and arteriovenous shunting [19], we did not use crusher gradients. Stack-of-spirals 3D fast spin echo imaging is insensitive to susceptibility MRI artifacts [21] and it may attenuate susceptibility artifacts from bone in the skull base. Diagnostically it may therefore be superior to the susceptibility vessel sign on T2*-gradient echo images.

Our study has some limitations. As we included only patients with angiographically-confirmed acute ICA occlusion, our sample size was small and we cannot exclude bias in the analysis of retrospective data. Although there were no false-positive findings, such results can be obtained in patients with severe ICA stenosis. Since IASs represent slow antegrade arterial flow, in patients with severe stenosis they may be visible in a distal segment. Our findings should be confirmed in a large cohort.

Also, the therapeutic intervention procedures may have affected the hemodynamics. Nonetheless, we confirmed that symptoms of all patients did not change from the MRI to the angiography in this study.

Conclusions

We show that IASs on ASL images can be used to identify the sites of slow stagnant- and collateral flow in patients with acute ICA occlusion. Our findings confirm the high sensitivity, specificity, and accuracy of IASs in the C1-C2 segments for a diagnosis of acute intracranial ICA occlusion. Additional studies are underway to determine the usefulness of IAS detection for the diagnostic work-up and treatment of patients with ischemic stroke.

References

1. Paciaroni M, Balucani C, Agnelli G, Caso V, Silvestrelli G, Grotta JC, Demchuk AM, Sohn SI, Orlandi G, Leys D, Pezzini A, Alexandrov AV, Silvestrini M, Fofi L, Barlinn K, Inzitari D, Ferrarese C, Tassi R, Tsivgoulis G, Consoli D, Baldi A, Bovi P, Luda E, Galletti G, Invernizzi P, DeLodovici ML, Corea F, Del Sette M, Monaco S, Marcheselli S, Alberti A, Venti M, Acciarresi M, D'Amore C, Macellari F, Lanari A, Previdi P, Gonzales NR, Pandurengan RK, Vahidy FS, Sline M, Bal SS, Chiti A, Gialdini G, Dumont F, Cordonnier C, Debette S, Padovani A, Cerqua R, Bodechtel U, Kepplinger J, Nesi M, Nencini P, Beretta S, Trentini C, Martini G, Piperidou C, Heliopoulos I, D'Anna S, Cappellari M, Donati E, Bono G, Traverso E, Toni D (2012) Systemic thrombolysis in patients with acute ischemic stroke and Internal Carotid ARtery Occlusion: the ICARO study. Stroke 43:125-130
2. Berkhemer OA, Fransen PS, Beumer D, van den Berg LA, Lingsma HF, Yoo AJ, Schonewille WJ, Vos JA, Nederkoorn PJ, Wermer MJ, van Walderveen MA, Staals J, Hofmeijer J, van Oostayen JA, Lycklama a Nijeholt GJ, Boiten J, Brouwer PA, Emmer BJ, de Bruijn SF, van Dijk LC, Kappelle LJ, Lo RH, van Dijk EJ, de Vries J, de Kort PL, van Rooij WJ, van den Berg JS, van Hasselt BA, Aerden LA, Dallinga RJ, Visser MC, Bot JC, Vroomen PC, Eshghi O, Schreuder TH, Heijboer RJ, Keizer

K, Tielbeek AV, den Hertog HM, Gerrits DG, van den Berg-Vos RM, Karas GB, Steyerberg EW, Flach HZ, Marquering HA, Sprengers ME, Jenniskens SF, Beenen LF, van den Berg R, Koudstaal PJ, van Zwam WH, Roos YB, van der Lugt A, van Oostenbrugge RJ, Majoie CB, Dippel DW (2015) A randomized trial of intraarterial treatment for acute ischemic stroke. N Engl J Med 372:11-20

3. Campbell BC, Mitchell PJ, Kleinig TJ, Dewey HM, Churilov L, Yassi N, Yan B, Dowling RJ, Parsons MW, Oxley TJ, Wu TY, Brooks M, Simpson MA, Miteff F, Levi CR, Krause M, Harrington TJ, Faulder KC, Steinfort BS, Priglinger M, Ang T, Scroop R, Barber PA, McGuinness B, Wijeratne T, Phan TG, Chong W, Chandra RV, Bladin CF, Badve M, Rice H, de Villiers L, Ma H, Desmond PM, Donnan GA, Davis SM (2015) Endovascular therapy for ischemic stroke with perfusion-imaging selection. N Engl J Med 372:1009-1018

4. Goyal M, Demchuk AM, Menon BK, Eesa M, Rempel JL, Thornton J, Roy D, Jovin TG, Willinsky RA, Sapkota BL, Dowlatshahi D, Frei DF, Kamal NR, Montanera WJ, Poppe AY, Ryckborst KJ, Silver FL, Shuaib A, Tampieri D, Williams D, Bang OY, Baxter BW, Burns PA, Choe H, Heo JH, Holmstedt CA, Jankowitz B, Kelly M, Linares G, Mandzia JL, Shankar J, Sohn SI, Swartz RH, Barber PA, Coutts SB, Smith EE, Morrish WF, Weill A, Subramaniam S, Mitha AP, Wong JH, Lowerison

MW, Sajobi TT, Hill MD (2015) Randomized assessment of rapid endovascular treatment of ischemic stroke. N Engl J Med 372:1019-1030

5. Saver JL, Goyal M, Bonafe A, Diener HC, Levy EI, Pereira VM, Albers GW, Cognard C, Cohen DJ, Hacke W, Jansen O, Jovin TG, Mattle HP, Nogueira RG, Siddiqui AH, Yavagal DR, Baxter BW, Devlin TG, Lopes DK, Reddy VK, du Mesnil de Rochemont R, Singer OC, Jahan R (2015) Stent-retriever thrombectomy after intravenous t-PA vs. t-PA alone in stroke. N Engl J Med 372:2285-2295
6. Kwak JH, Zhao L, Kim JK, Park S, Lee DG, Shim JH, Lee DH, Kim JS, Suh DC (2014) The outcome and efficacy of recanalization in patients with acute internal carotid artery occlusion. AJNR Am J Neuroradiol 35:747-753
7. Bokkers RP, Hernandez DA, Merino JG, Mirasol RV, van Osch MJ, Hendrikse J, Warach S, Latour LL (2012) Whole-brain arterial spin labeling perfusion MRI in patients with acute stroke. Stroke 43:1290-1294
8. Griebe M, Kern R, Eisele P, Sick C, Wolf ME, Sauter-Servaes J, Gregori J, Gunther M, Hennerici MG, Szabo K (2013) Continuous magnetic resonance perfusion imaging acquisition during systemic thrombolysis in acute stroke. Cerebrovasc Dis 35:554-559

9. Detre JA, Samuels OB, Alsop DC, Gonzalez-At JB, Kasner SE, Raps EC (1999) Noninvasive magnetic resonance imaging evaluation of cerebral blood flow with acetazolamide challenge in patients with cerebrovascular stenosis. J Magn Reson Imaging 10:870-875
10. Yoo RE, Yun TJ, Rhim JH, Yoon BW, Kang KM, Choi SH, Kim JH, Kim JE, Kang HS, Sohn CH, Han MH (2015) Bright vessel appearance on arterial spin labeling MRI for localizing arterial occlusion in acute ischemic stroke. Stroke 46:564-567
11. Majer M, Mejdoubi M, Schertz M, Colombani S, Arrigo A (2015) Raw arterial spin labeling data can help identify arterial occlusion in acute ischemic stroke. Stroke 46:e141-144
12. Junya A, Kazumi K, Kensaku S, Yuki S (2013) DWI-ASPECTS as a predictor of dramatic recovery after intravenous recombinant tissue plasminogen activator administration in patients with middle cerebral artery occlusion. Stroke 44:534-537
13. Adams HP, Jr., Bendixen BH, Kappelle LJ, Biller J, Love BB, Gordon DL, Marsh EE 3rd (1999) Classification of subtype of acute ischemic stroke. Definitions for use in a multicenter clinical trial. TOAST. Trial of Org 10172 in Acute Stroke Treatment. Stroke 24:35-41

14. Dai W, Garcia D, de Bazelaire C, Alsop DC (2008) Continuous flow-driven inversion for arterial spin labeling using pulsed radio frequency and gradient fields. Magn Reson Med 60:1488-1497

15. Gibo H, Lenkey C, Rhoton AL Jr (1981) Microsurgical anatomy of the supraclinoid portion of the internal carotid artery. J Neurosurg 55:560-574

16. Tada Y, Satomi J, Abe T, Kuwayama K, Sogabe S, Fujita K, Yamamoto N, Kaji R, Harada M, Nagahiro S (2014) Intra-arterial signal on arterial spin labeling perfusion MRI to identify the presence of acute middle cerebral artery occlusion. Cerebrovasc Dis 38:191-196

17. Morita N, Harada M, Uno M, Matsubara S, Matsuda T, Nagahiro S, Nishitani H (2008) Ischemic findings of T2*-weighted 3-tesla MRI in acute stroke patients. Cerebrovasc Dis 26:367-375

18. Zaharchuk G (2012) Arterial spin labeling for acute stroke: practical considerations. Transl Stroke Res 3:228-235

19. Alsop DC, Detre JA, Golay X, Günther M, Hendrikse , Hernandez-Garcia L8, Lu H, MacIntosh BJ, Parkes LM, Smits M, van Osch MJ, Wang DJ, Wong EC, Zaharchuk G (2015) Recommended implementation of arterial spin-labeled perfusion MRI for

clinical applications: A consensus of the ISMRM perfusion study group and the European consortium for ASL in dementia. Magn Reson Med. 73:102-116

20. Wang DJ, Alger JR, Qiao JX, Gunther M, Pope WB, Saver JL, Salamon N, Liebeskind DS; UCLA Stroke Investigators (2013) Multi-delay multi-parametric arterial spin-labeled perfusion MRI in acute ischemic stroke - Comparison with dynamic susceptibility contrast enhanced perfusion imaging. Neuroimage Clin. 3:1-7

21. Liu TT, Brown GG (2007) Measurement of cerebral perfusion with arterial spin labeling: Part 1. Methods. J Int Neuropsychol Soc 13:517-525

Figure Legends

Fig. 1

Representative angiographic- and MRI findings in a patient with ICA occlusion at the C4 segment

A 70-year-old man presented with aphasia and right hemiparesis (case 3).

A: DWI (a) and ASL (b) indicated a large penumbral area.

- a: High-intensity signals in the insula, anterior MCA cortex, and anterior MCA territory (DWI-ASPECTS: 8).
- b: ASL showed reduced perfusion in all of the MCA territory.

B: Early- (a) and late phase (b) of left common carotid angiography and schema of the occlusion site and the blood flow (c).

- a: Left common carotid angiograph showing patency at the origin of the ICA (arrow).
- b: In the late phase of left common carotid angiography there is slow stagnant flow along the ICA from the C4- to the C1 segment (arrows).
- c: Schema of the blood flow seen on digital subtraction angiographs (black arrow, blood flow; solid portion, occlusion site).

C: Upper panels, ASL; lower panels, MRA of the ICA on the normal side (the lines correspond with the ASL image). ASL shows IASs in the left ICA in segments C4 (a), C3 (b), C2 (c), and C1 (d). (IAS: arrow)

D: Schema of ASL images (the occlusion site is solid, the IAS-positive segment is hatched).

Fig. 2

Representative angiographic- and MRI findings in a patient with ICA occlusion at the C3 segment

An 81-year-old woman presented with aphasia and consciousness disturbance (case 6).

A: DWI (a) and ASL (b) indicated a large penumbral area.

- a: High intensity signals were shown in the lenticular nucleus (DWI-ASPECTS: 10).
- b: ASL showed reduced perfusion in all of the MCA territory.

B: Early- (a) and late phase (b) of left common carotid angiography and schema of the occlusion site and blood flow (c).

- a: Left common carotid angiograph showing patency at the origin of the ICA (arrow).

b: In the late phase of left common carotid angiography there is collateral flow into the C4 segment of the ICA through the ophthalmic artery (arrow).

c: Schema of the blood flow seen on DSA images (black arrow, blood flow; solid portion, occlusion site).

C: Upper panels, ASL; lower panels, MRA of the ICA on the normal side (the lines correspond with the ASL image). ASL shows IASs in the left ICA in segment C4 (a). (IAS: arrow)

D: Schema of ASL images (the occlusion site is solid, the IAS-positive segment is hatched).

Fig. 3

Representative angiographic- and MRI findings in a patient with extracranial ICA occlusion

An 84-year-old man with a history of symptomatic left ICA stenosis presented with aphasia and right hemiparesis (case 8).

A: DWI (a) and ASL (b) indicated a large penumbral area.

a: High intensity signals were shown in the insula ribbon, the MCA cortex lateral to the insula ribbon, and the lateral MCA territory (DWI-ASPECTS: 8).

b: ASL showed reduced perfusion in all of the MCA territory.

B: Left common carotid angiograph obtained before (a) and after balloon angioplasty (b) and schema of the occlusion site and blood flow (c).

a: Occlusion at the origin of the ICA and collateral flow through the ophthalmic artery (arrow).

b: Left ICA stenosis (arrow).

c: Schema of the blood flow seen on DSA images (black arrow, blood flow; solid portion, occlusion site).

C: Upper panels, ASL; lower panels, MRA of the ICA on the normal side (the lines correspond with the ASL image). ASL shows IASs in the left ICA in segments C4 (a) and C3 (b). (IAS: arrow)

D: Schema of ASL images (the occlusion site is solid, the IAS-positive segment is hatched).

Fig. 4

The number of IAS-positive slices and segments in each patient

The occluded segment in patients 1-7 was in the intracranial ICA (1-5: C4 segment; 6 and 7: lower than the C3 segment). The occluded segment in patients 8-13 was the extracranial ICA. Although 5 of 7 patients with intracranial ICA occlusion had IASs at segments C1 and C2, no IASs were observed at C1 and C2 in patients with extracranial ICA occlusion. The number of IAS-positive slices on ASL images was significantly higher in patients with intracranial- than extracranial ICA occlusion (average 8.3 vs. 2.0 slices: $p < 0.05$). Data were analyzed with the Mann-Whitney *U*-test.

Table 1

Patients and treatments

Case No	Age, Sex	Initial NIHSS	Etiology	Onset to MRI (minutes)	DWI-ASPECTS	IV tPA therapy	Occlusion segment*	ICA flow arrest	Past History	Endovascular procedure
1	88, M	11	ATBI	701	11	-	C4,M1distal	-	HT	Balloon angioplasty
2	75, M	21	CE	645	6	-	C4	-	HT, AF	Penumbra
3	70, M	18	CE	269	8	-	C4	-	AF	Merci→Penumbra
4	86, F	16	CE	406	8	-	C4	-	HT, AF, DL	Penumbra
5	67, M	13	CE	305	10	-	C4-M1 proximal	-	HT,DM	Trevo
6	81, F	15	other**	632	10	-	C3	+	HT, DM	Penumbra→Trevo
7	90, M	10	CE	323	11	-	C3-M1 proximal	+	HT	Trevo
8	84, M	16	ATBI	602	8	-	C1, M1 distal		HT	CAS→Penumbra
9	76, M	12	CE	1640	11	-	C1-C3		HT, AF	Penumbra
10	73, M	14	ATBI	261	8	-	C1, M1 distal		DL	CAS→Solitaire
11	67, F	28	ATBI	75	8	+	C1, M1 distal		-	CAS→Penumbra
12	78, M	23	ATBI	654	9	-	C1, M1 proximal		HT, DM	CAS→Penumbra
13	55, M	10	ATBI	83	11	+	C1, C4		-	CAS→Penumbra

*Includes long and tandem lesions.

**Embolism based on the Trousseau syndrome

Abbreviations: ATBI, atherothrombotic brain infarction; DWI-ASPECTS, diffusion weighted imaging - the Alberta Stroke Program Early Computed Tomography Score; AF, atrial fibrillation; C1, supraclinoid-, C2, cavernous-, C3, petrous-, C4, cervical segment of the ICA; CAS, carotid artery stenting [penumbra, aspiration system (Penumbra Alameda), Merci, Merci retriever system (Concentric Medical, Mountain View), Trevo, stent retriever system (Stryker Neurovascular), Solitaire, stent retriever system (eV3

Neurovascular)]; CE, cardioembolism; DL, dyslipidemia; DM, diabetes mellitus; HT, hypertension; M1, middle cerebral artery, horizontal segment

Table 2 Value of IASs on ASL images for diagnosing intracranial ICA occlusion

Assessment of IAS at the C1-C2 segments in ICA		
	n	%
Sensitivity	5/7	71
Specificity	6/6	100
Positive predictive value	5/5	100
Negative predictive value	6/8	75
Accuracy	11/13	85

The incidence of IAS-positive C1 and C2 segments was significantly higher in patients with intra- than extracranial ICA occlusion (5/7 vs. 0/6).

Fig. 1

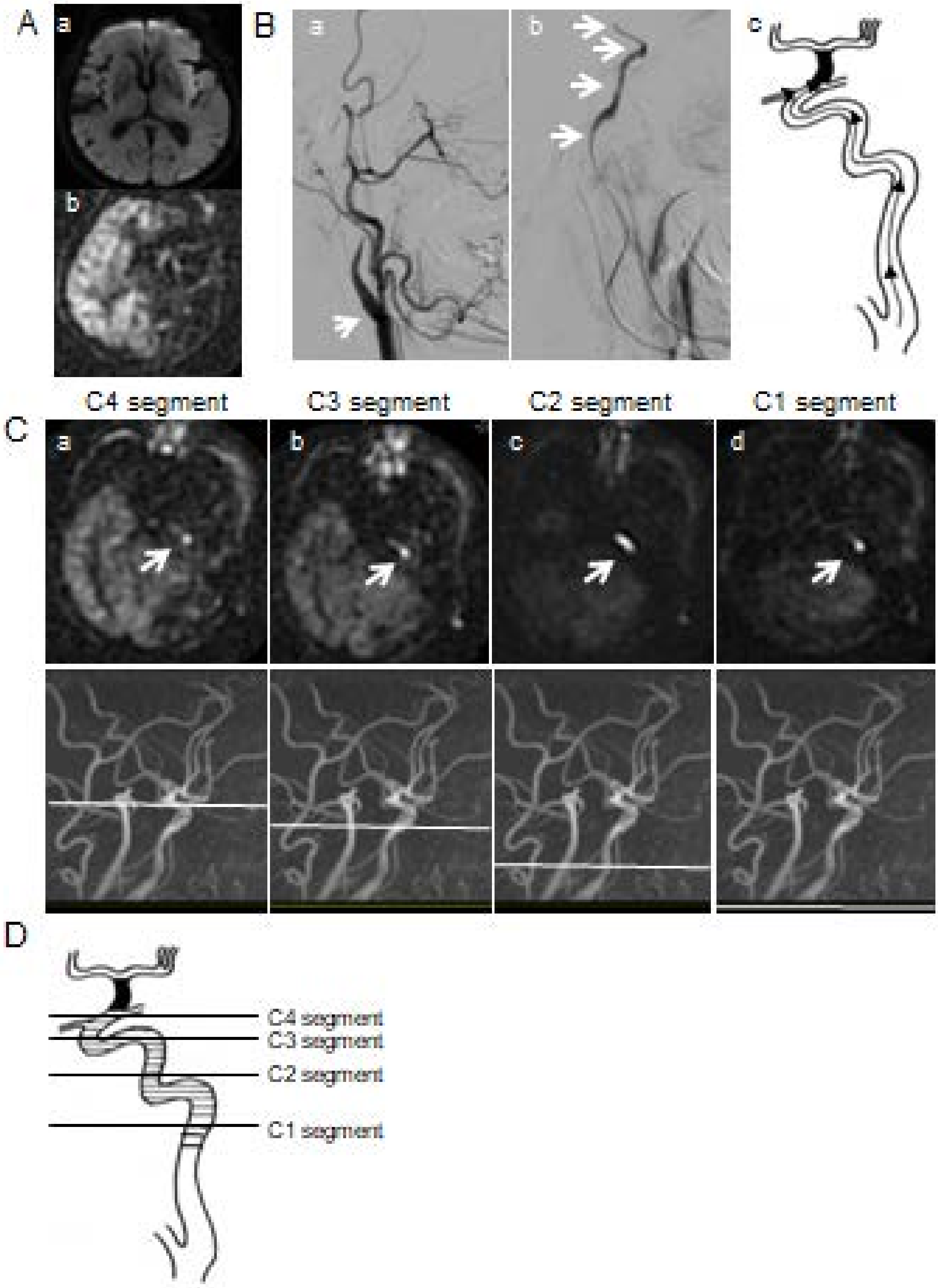
A
a
b
B
a
b
c
C4 segment
C3 segment
C2 segment
C1 segment
C
a
b
c
d
D
C4 segment
C3 segment
C2 segment
C1 segment

Fig. 2

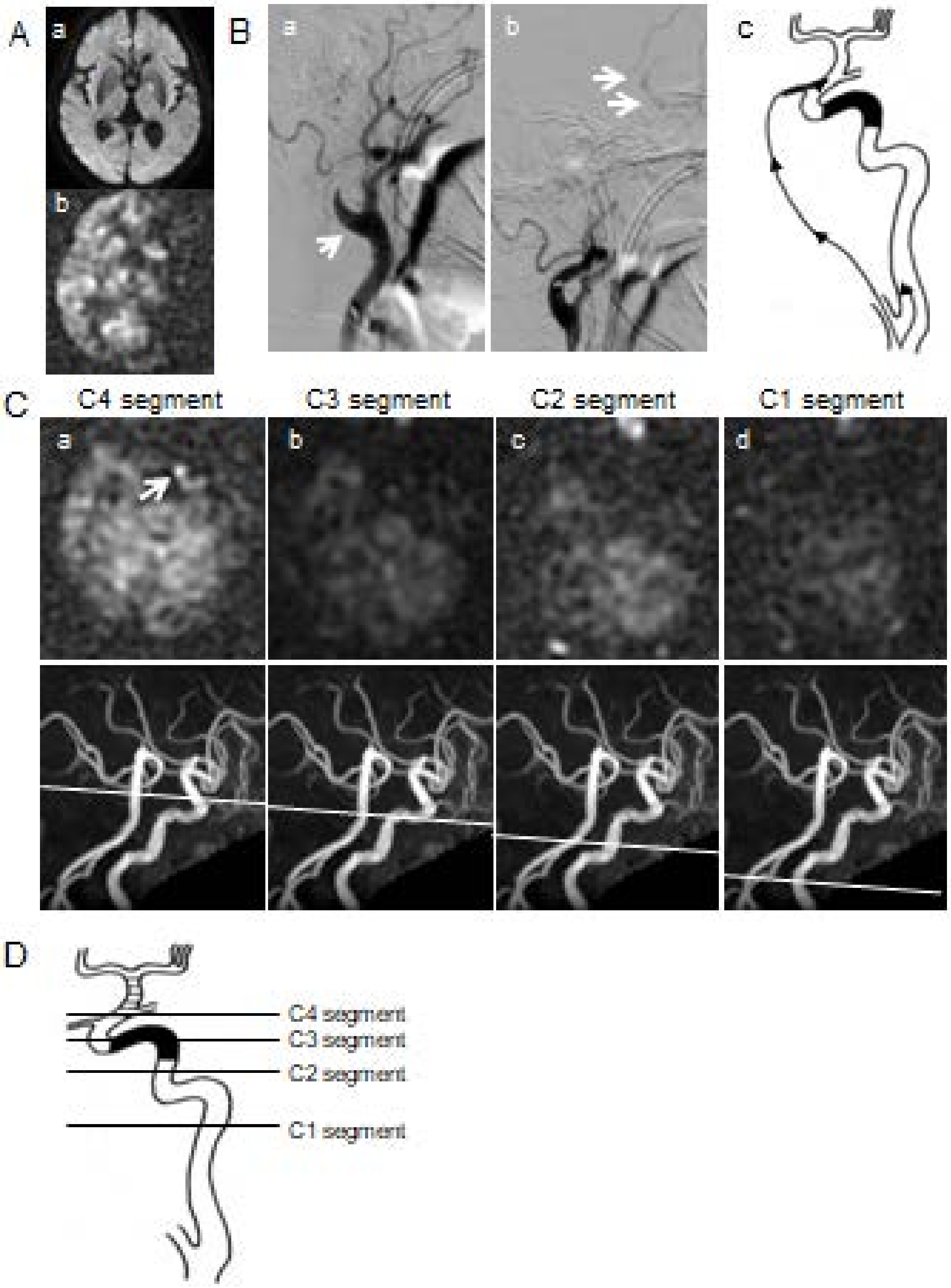
A
a
b
B
a
b
c
C
C4 segment
C3 segment
C2 segment
C1 segment
a
b
c
d
D
C4 segment
C3 segment
C2 segment
C1 segment

Fig. 3

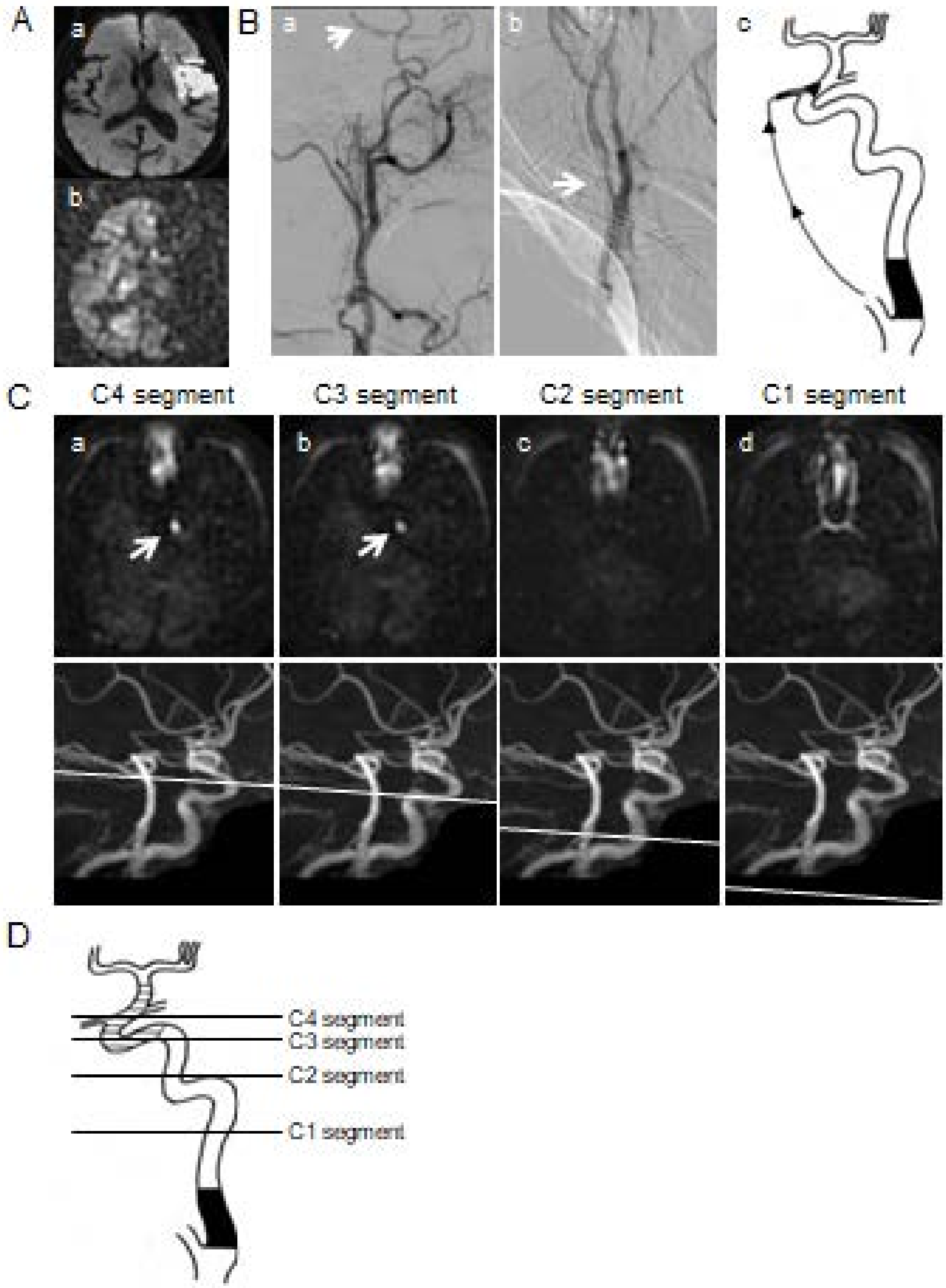
A
a
b
B
a
b
c
C
C4 segment
C3 segment
C2 segment
C1 segment
a
b
c
d
D
C4 segment
C3 segment
C2 segment
C1 segment

1

2

Fig. 4

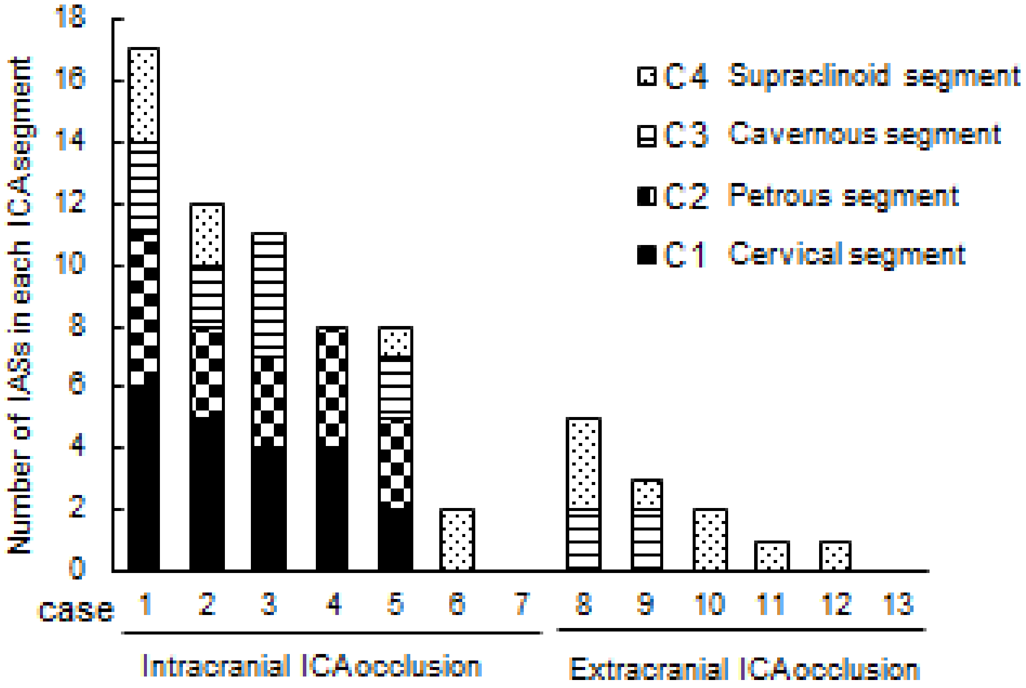

Number of IASs in each ICA segment
18
16
14
12
10
8
6
4
2
0
case
1
2
3
4
5
6
7
8
9
10
11
12
13
Intracranial ICA occlusion
Extracranial ICA occlusion
C4 Supraclinoid segment
C3 Cavernous segment
C2 Petrous segment
C1 Cervical segment

1